ARTICLE

BIOTECHNOLOGY and BIOENGINEERING

Triterpene Hydrocarbon Production Engineered Into a Metabolically Versatile Host—*Rhodobacter capsulatus*

Nymul E. Khan,[1] S. Eric Nybo,[2] Joe Chappell,[2] Wayne R. Curtis[1]

[1]Department of Chemical Engineering, The Pennsylvania State University, University Park, Pennsylvania 16802; telephone: 814-863-4805; fax: 814-865-7846; e-mail: wrc2@psu.edu

[2]Department of Pharmaceutical Sciences, University of Kentucky, Lexington, Kentucky 40536

ABSTRACT: Triterpene hydrocarbon biosynthesis of the ancient algae *Botryococcus braunii* was installed into *Rhodobacter capsulatus* to explore the production of C_{30} hydrocarbon in a host capable of diverse growth habits—utilizing carbohydrate, sunlight or hydrogen (with CO_2 fixation) as alternative energy feedstocks. Engineering an enhanced MEP pathway was also used to augment triterpene accumulation. Despite dramatically different sources of carbon and reducing power, nearly the same level of botryococcene or squalene (~5 mg oil/g-dry-weight [gDW]) was achieved in small-scale aerobic heterotrophic, anaerobic photoheterotrophic, and aerobic chemoautotrophic growth conditions. A glucose fed-batch bioreactor reached 40 mg botryococcene/L (~12 mg/gDW), while autotrophic bioreactor performance with CO_2, H_2, and O_2 reached 110 mg/L (16.7 mg/gDW) during batch and 60 mg/L (23 mg/gDW) during continuous operation at a dilution rate corresponding to about 10% of μ_{max}. Batch and continuous autotrophic specific productivity was found to reach 0.5 and 0.32 mg triterpene/g DW/h, comparable to prior reports for terpene production driven by heterotrophic growth conditions. This demonstrates the feasibility of alternative feedstocks and trophic modes to provide comparable routes to biochemicals that do not rely on sugar.

Biotechnol. Bioeng. 2015;112: 1523–1532.

© 2015 Wiley Periodicals, Inc.

KEYWORDS: CO_2 fixation; squalene; botryococcene; MEP pathway; productivity; continuous bioreactor

Introduction

Feedstock flexibility is being pursued to improve the economic feasibility and sustainability of the production of biofuels and chemicals. Corn-ethanol and the ongoing transitioning to cellulosic-ethanol or biobutanol are examples of allowing plants to capture photonic energy in chemical bonds, and subsequently releasing that energy to selectively produce a more convenient liquid transportation fuel. Similarly, the production of biofuels by algae reflects an even more direct use of the sun that relies on the storage of triacylglycerol lipids by these photosynthetic organisms. These oils can then be converted to biodiesel with minimum processing requirements. The use of these plant-derived energy sources, is inherently competitive with their alternative use as food and adds to the interaction of energy and food production costs. A more desirable alternative would be a host organism capable of chemical production from a variety of energy and carbon sources. To demonstrate this, we have targeted the production of two C_{30} hydrocarbons, a biofuel (botryococcene), and a pharmaceutical constituent (squalene)—botryococcene and squalene, in *Rhodobacter capsulatus*—a host capable of diverse metabolism and robust growth.

Nature has devised extensive options to tap into the energy of the sun, with equally diverse carbon balances. This presents alternative approaches for biofuels production, where Figure 1 illustrates the metabolic scenarios addressed in the presented work. Heterotrophic growth is the familiar consumption of carbohydrates, where aerobic growth takes advantage of metabolic efficiencies to produce CO_2 and water. When oxygen is constrained, anaerobic heterotrophic metabolism can result in the production of alcohols and organic acids and dihydrogen gas. Photoheterotrophic metabolism utilizes a carbon source such as malic or succinic acid from the TCA cycle and achieves tremendous carbon-use efficiency by generating most of its energy by ATP production from photophosphorylation. The final *R. capsulatus* trophism illustrated in Figure 1 is aerobic chemolithoautotrophic metabolism, where the photonic energy generates hydrogen (via electrolytic splitting of water), and this energy can then be used to fix carbon dioxide. In nature the CO_2 and H_2 can be derived from anaerobic metabolism.

Current address of S. Eric Nybo is Department of Pharmaceutical Sciences, College of Pharmacy, Ferris State University, Big Rapids, MI, USA.
Nymul Khan and S. Eric Nybo contributed equally to this work.
Correspondence to: W. R. Curtis
Contract grant sponsor: U.S. Department of Energy
Contract grant number: ARPA-e Electrofuels, DE-AR0000092
Received 31 October 2014; Revision received 14 January 2015; Accepted 11 February 2015
Accepted manuscript online 27 February 2015;
Article first published online 12 May 2015 in Wiley Online Library (http://onlinelibrary.wiley.com/doi/10.1002/bit.25573/abstract).
DOI 10.1002/bit.25573

© 2015 Wiley Periodicals, Inc.

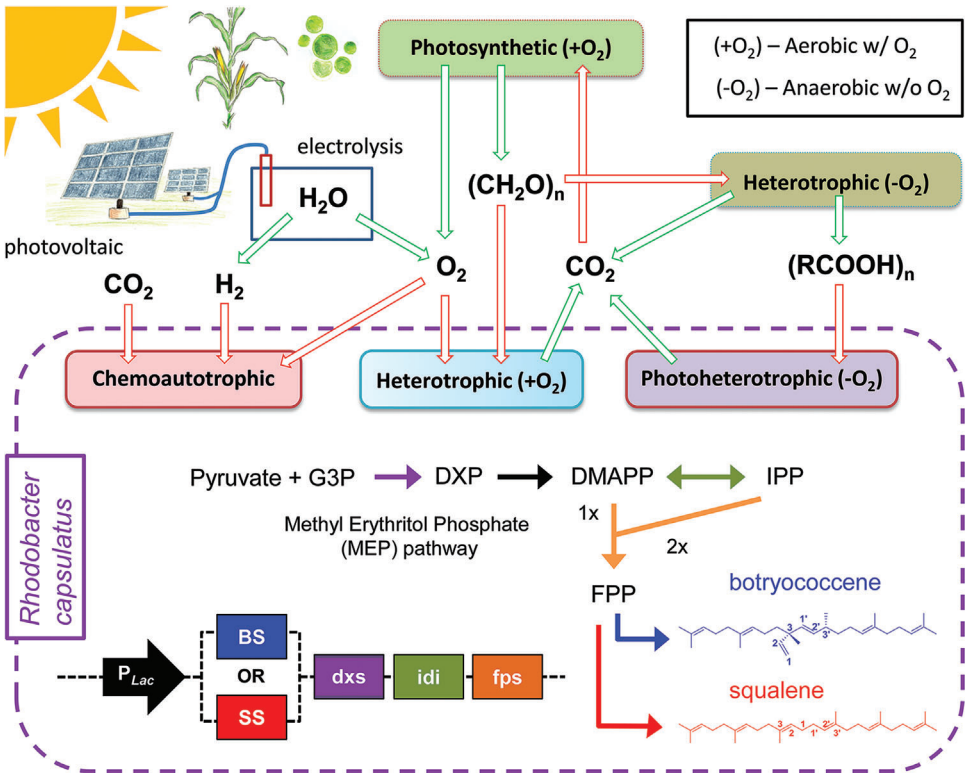

Figure 1. *Rhodobacter capsulatus* is a metabolically diverse organism that can utilize and interconvert the energy provided from the sun in a variety of different ways. Metabolism within the dashed line representing *Rhodobacter* cell are those reported in this study: aerobic chemoautrophic growth consumes H_2 and O_2 while fixing CO_2, with these gases being provided by photovoltaic-driven electrolysis in this scenario (or other natural sources). Aerobic heterotrophic growth is the typical consumption of sugars and associated aerobic respiration, anaeobic photoheterotrophic growth consumes energy poor organic acids with photosystem-II mediated ATP generation using light energy. Depiction of the evolution (green arrows) or uptake (red arrows) of metabolic gases emphasizes the bioreactor requirements for gas-exchange as a major constraint for process design and operation. The lower part of the figure depicts the metabolic engineering strategy within the *Rhodobacter* cell to achieve the production of the high energy terpenes botryococcene or squalene. The DNA construct includes the genes for the enzyme that commits carbon flux to the MEP pathway: (1-Deoxy-D-xylulose 5-phosphate synthase, *dxs*) and the isopentenyl diphosphate (IPP) isomerase (*idi*) that enhances the ratio of IPP to dimethylallyl pyrophosphate (DMAPP). This construct also includes the gene for farnesyl diphosphate synthase (*fps*) which utilizes one DMAPP and two IPP to produce C15 farnesyl pyrophosphate, the substrate for the terpene synthases (botryococcene synthase, BS; squalene synthase, SS).

The options available for biofuel product molecule expands upon feedstock flexibility to present innumerable options for proposed biochemical production platforms. Our work focuses on the triterpene hydrocarbons (C_{30+}), squalene and botryococcene, because of their higher energy density than ethanol (Tuerk, 2011) and ability to be processed nearly identically to that of crude oil (Hillen et al., 1982). Most notable from a process design perspective is that the hydrocarbon fuels are sufficiently hydrophobic to phase-separate, thereby eliminating the energy-intensive distillation step that constrains the ethanol production processes. The specific choice of botryococcene from the colonial algae *Botryococcus braunii* race B was motivated in part by the observation that this is one of the few biomolecules known to directly contribute up to 1% of all oil shales (Derenne et al., 1997; Glikson et al., 1989). In its native algal host, botryococcene oils are unique as compared to other photosynthetic algae associated with biofuels production (Metzger and Largeau, 2005). These oils are not for energy storage; their apparent use for floatation results in their production to exceeding high levels >30% of the carbon budget that is independent of the growth rate (Khatri et al., 2014). As a result, they accumulate at all stages of growth, and are not limited to growth-attenuated storage conditions that characterize most algae biofuels scenarios. We previously isolated the genes for the biosynthesis of botryococcene and characterized their unusual biosynthetic mechanisms (Niehaus et al., 2011; Wu et al., 2012). This understanding has led to the generation of the functional chimeric botryococcene synthase (*BS*) gene used in this work. The more direct biosynthetic route to squalene, another linear triterpene analog to botryococcene, was also compared using the squalene synthase (*SS*) gene from the same *B. braunii* host as illustrated in Figure 1. The work presented here therefore combines the concept of feedstock flexibility with the production of advanced hydrocarbon biofuels. The multi-trophic utilization of feedstocks for hydrocarbon biofuels production introduces constraints and opportunities for bioprocess engineering. Within the production bioreactor, gas exchange is a dominant consideration due to the low solubility of gases in aqueous solution and the energy required to transport these gases across the interface. The familiar aerobic heterotrophic reactor has oxygen uptake and CO_2 evolution, which is the opposite of the oxygenic photosynthetic algae. The less familiar anaerobic photoheterotrophic condition has minimal gas transport considerations due to only minor CO_2 evolution, but has a

large photon flux requirement. Aerobic chemolithoautotrophic metabolism fixes CO_2, using H_2 as electron donor and therefore has the greatest requirements for gas transport of the presented options. At the same time, since gas transport is unidirectional (into the culture), chemolithoautotrophic growth can be performed with 100% conversion of the gas phase (Bongers, 1970), which enables the most efficient utilization of the gas feedstocks presented. Our choice of the purple photosynthetic bacteria *R. capsulatus* therefore provides great latitude for examining diverse modes of feedstock metabolism to triterpenes in the same organism.

In this study, we generated plasmid DNA constructs to produce C_{30} squalene and botryococcene in *R. capsulatus* that are shown to have sufficient activity to be limited by substrate availability. We then characterize the triterpene productivity for the three trophic modes of aerobic heterotrophic, anaerobic photoheterotrophic, and aerobic chemoautotrophic metabolism. Finally, we demonstrate the ability to further improve productivity by operating under fed-batch and continuous production conditions in heterotrophic and autotrophic stirred tank bioreactors.

Materials and Methods

Bacterial Strains and Growth Conditions

E. coli DH5α (Invitrogen) was used as the host for routine cloning experiments and for *E. coli* triterpene engineering. *E.coli* DH5α was grown on LB agar or in LB broth at 37 °C for cloning and routine maintenance. For triterpene engineering, *E. coli* DH5α was transformed with the plasmid constructs using standard heat shock protocols (Schmidt et al., 1999). *Rhodobacter capsulatus* SB1003 (ATCC BAA-309) was used as a second prokaryotic host for triterpene engineering experiments. For heterotrophic growth and maintenance, *Rhodobacter capsulatus* was grown in YCC (Sistrom, 1977) liquid medium and on YCC agar plates at 34 °C. When phosphate buffered saline was required, phosphates were added to a final concentration of 6.60 mM K_2HPO_4, 3.30 mM KH_2PO_4 just before inoculation. Glucose supplementation was accomplished by, adding a sterilized 1 M glucose solution to a final concentration of 20–100 mM just before inoculation. The bacterial cell lines are described in (Supplementary Table 1). When appropriate, *E. coli* strains were grown with 50 $\mu g\,mL^{-1}$ kanamycin and 100 $\mu g\,mL^{-1}$ ampicillin. *R. capsulatus* strains were grown in the presence of 20 $\mu g\,mL^{-1}$ kanamycin and 10 $\mu g\,mL^{-1}$ rifampicin.

For heterotrophic production of triterpenes, both *E. coli* and *R. capsulatus* were picked as a single colony from a plate and grown in 1 mL of LB or YCC, respectively and were incubated for 20 h at 37 °C or 34 °C. This allowed for normalization of growth between biological replicates the same growth-stage before performing the time course and terminal endpoint fermentations. Terminal endpoints for heterotrophic and photoheterotrophic samples were taken after 48 h for five replicate cultures.

Small Scale Phototrophic and Autotrophic Growth Conditions for *R. capsulatus* Strains

To induce photoheterotrophic growth, *Rhodobacter capsulatus* SB1003 wildtype strain and its derivatives were picked as single colonies directly from YCC conjugation plates (supplemented with antibiotics when appropriate) and inoculated into 13 mm screw cap culture tubes filled completely with RCVB medium (Madigan and Gest, 1979). This photoheterotrophic growth phase was found to be necessary to efficiently transition *R. capsulatus* SB1003 from chemoheterotrophic growth to autotrophic growth. The cells were grown anaerobically under light to saturation and inoculated to a starting OD_{660} of about 0.1 (Beckman DU520 spectrophotometer) into CA medium (Madigan and Gest, 1979) with antibiotics. After the lag period, 2 mL samples are removed every 24 h to measure OD_{660} and analyze for product.

The input gases for autotrophic growth (H_2, CO_2, and O_2) were mixed via three mass flow controllers (SLA5850, Brooks Instruments, Hatfield, PA) to a set composition of 80:10:10. The autotrophic growth setup consists of 125 mL baffled Erlenmeyer flasks, each with a gas inlet and outlet, and a sampling port (5" 16G needle extending to the bottom of flask with 3 mL syringe). The flasks are connected in series for gas delivery and are shaken at 200 rpm (G2 shaker, New Brunswick). The entire setup is contained in an incubated chamber kept at 34 °C.

Heterotrophic Bioreactor Growth Condition

Cells were grown in a 5 L bioreactor (BioFlo, New Brunswick, Edison, NJ) with a two Rushton impellers in glucose fed-batch mode. The working liquid volume of the reactor was 4 L. The pH of the culture was maintained at 7 by feeding 8 N NH_4OH solution. The O_2 fraction in the gas feed and the agitation was increased manually initially to maintain dissolved oxygen (DO) around 20% of air saturation until an RPM of 250 and O_2 fraction of 15%. Temperature was maintained at 34°C. The reactor was inoculated from a 100 mL shake-flask culture grown aerobic heterotrophically in RCVB (-Malate) media + 80 mM glucose + 25 μg/mL kanamycin to a starting OD_{660} of around 0.1 in the reactor of the same media (Madigan and Gest, 1979). Two to three milliliter sample was removed from the reactor at regular interval for the measurement of OD_{660} and hydrocarbon content.

Autotrophic Bioreactor Growth Conditions

Cells were grown in a 1 L bioreactor (BioFlo, New Brunswick, Edison, NJ) with a cell-lift impeller in batch and continuous growth mode. The working liquid volume of the reactor was 900 mL. The inlet gas stream was mixed using three high-precision mass flow controllers (SLA5850, Brooks Instruments, Hatfield, PA) and the outlet gas flow rate and compositions were measured using a mass flow meter (M-50SCCM-D, Alicat Scientific, Tucson, AZ) and two gas flow sensors for H_2 and O_2/CO_2, respectively (BlueSens, Herten, Germany). The pH of the culture was maintained at 7 by feeding 25% NH_4OH solution. The RPM and temperature were maintained at 1,000 and 34°C. The inlet gas flow rate and compositions were varied during batch growth but kept constant during continuous growth mode (discussed in the results section). The reactor was inoculated from an autotrophically grown flask culture (described above) to a starting OD_{660} of 0.1 in CA media with antibiotic (Imam et al., 2013). After about 15 h from inoculation, 2 mL sample was removed from the reactor at a regular interval for the measurement of OD_{660} and hydrocarbon.

Cloning Procedures

Nucleotide sequences for the native and codon optimized versions of genes used in this report are included in (Supplementary Table 2). The *Rhodobacter* codon optimized genes were synthesized by Genscript. These genes were cloned into the pUC57 cloning vector and were the source of template for PCR amplification. All gene combinations were amplified from pUC57 templates by PCR according to standard procedures (Schmidt et al., 1999). Oligonucleotide primers are listed in (Supplementary Table 3). In brief, genes were amplified and spliced by overlap extension (SOE) into polycistronic cassettes, which were then cloned into pGEM-T-easy vector for sequencing (Promega). The outermost primer set for amplifying the fully spliced region was modified to have a unique 5′-*Bam*HI restriction site and a 3′-*Xba*I restriction site. The cassettes for *SS, BS, SS-fps, BS-fps, SS-dxs-idi-fps, and BS-dxs-idi-fps* were cut with unique *Bam*HI and *Xba*I restriction sites and spliced into the same sites of pBBR1MCS-2 under the control of the P_{Lac} promoter, which is a strong constitutive promoter in *R. capsulatus* due to the lack of the *lacI* repressor.

Intergeneric Mating Between *E. coli*S17-1 and *R. capsulatus* SB1003

E. coli S17-1 (ATCC 47055) was used as a host for intergeneric conjugation of pBBR1MCS-2 derivatives into *Rhodobacter capsulatus* SB1003 (Simon et al., 1983). In brief, *E. coli* S17-1 strains harboring the pBBR1MCS-2 derivative constructs was grown from a single colony in 1 mL of LB medium (supplemented with 50 $\mu g\,mL^{-1}$ kanamycin) to early log phase. In parallel, *R. capsulatus* SB1003 was grown in 1 mL of YCC (supplemented with 10 $\mu g\,mL^{-1}$ rifampicin) for 24 h before the conjugal mating experiment. The cells were spun down and washed twice with 1 mL of sterile LB, then the *E. coli* S17-1 donor and *R. capsulatus* recipient cells were each resuspended in 100 μL of sterile LB and mixed. The entire mating mixture was spot plated (10 μL) onto dried YCC agar plates and allowed to mate for 8–12 h. Matings were scraped with a toothpick, resuspended in 200 μL of sterile LB, and serially diluted onto YCC plates (supplemented with 10 $\mu g\,mL^{-1}$ rifampicin and 20 $\mu g\,mL^{-1}$ kanamycin) and incubated for 48–72 h before exconjugants appeared. Exconjugants were picked with a sterile toothpick and inoculated in 1 mL of YCC supplemented with antibiotics for 20 h so that all the strains were in early to middle stationary phase. These cultures were used to inoculate the shake flask and culture tube experiments.

Hydrocarbon Analysis

One mL of bacterial culture was mixed with 1 mL of acetone and 1 mL of hexane in a 4 mL glass vial and vortexed for 30 s to lyse the cells and to extract the triterpenes. The hexane phase was poured over a small silica column constructed in a Pasteur pipet (5 ¾" glass pipet, 0.8 g of Silica G60) previously wetted with n-hexane. The triterpene components were flushed through the column with nitrogen into a small 1.5 mL vial and washed with three column volumes of hexane to elute any bound triterpenes. The purified fraction was dried down under a gentle stream of nitrogen and resuspended in 100 μL for analysis on GC–MS (Niehaus et al., 2011). GC–MS analysis was conducted on an Agilent 7890 GC with an Agilent 5975 mass spec. Squalene standard (Sigma Aldrich) was analyzed in concentrations ranging from 1 ng to 100 ng to generate standard curves. Botryococcene standard was isolated from *Botryococcus braunii*.

Results

Achieving Substrate-Limited Triterpene Biosynthetic Constructs

To probe the productivity of *R. capsulatus* in various trophic modes, codon-optimized genetic constructs were assembled based on the triterpene target and known rate-limiting steps in biosynthesis of terpenes. Our recent work on botryococcene biosynthesis revealed a remarkable biochemical evolution where the triterpene botryococcene is synthesized by two separate enzyme homologs (Niehaus et al., 2011). This led to the generation of a chimeric fusion of these two sequentially acting enzymes, which provided the functional botryococcene synthase (BS) used in this work. For comparative purposes, the *B. braunii* squalene synthase (SS) is included which utilizes the same precursor as BS—farnesyl diphosphate (FPP) (Fig. 1). The avian FPP synthase (*fps*) gene was included in these constructs to ensure the robust production of the common FPP substrate (Wu et al., 2006). The genes encoding for the microbial equivalent of 1-deoxy-D-xylulose 5-phosphate synthase (*dxs*) and isoprenyl diphosphate isomerase (*idi*) were also included because of their known enhancement of carbon flux in the MEP pathway and to improve the stoichiometry for FPP formation (Miller et al., 2000).

The initial construction and functional testing of these constructs was carried out in *E. coli,* which achieved successively higher titers when the *dxs*,*idi,* and *fps* genes were added to the constructs (Supplementary Figures 1–3). Their performance in *R. capsulatus* for both squalene and botryococcene in heterotrophic mode is shown in Figure 2, confirming a requirement for *fps*, and the expected improved performance of the native squalene enzyme. However, the addition of *fps* was not sufficient to pull large carbon flux out of central metabolism. This limitation was relieved when the rate-limiting enzymes from the MEP pathway- *dxs* and *idi*- were added. Productivity increased by 20–100-fold over *fps*-only constructs. Further increases in productivity of 1.5–2 fold were observed when the medium (YCC) was supplemented with 80 mM glucose (Fig. 2b). This demonstrated that the introduced triterpene synthase activities were sufficient to be limited by general metabolic rates within central metabolism. The constructs containing the triterpene synthase and the enhanced MEP pathway components (pBBR:P_{lac}::*BS/SS-dxs-idi-fps*) were further utilized to probe for major differences in available flux from central metabolism under different trophic modes of growth.

The specific productivity at stationary phase for the different trophic growth modes were compared in small scale (<50 mL) cultures (Fig. 3a). Photoheterotrophic growth mode improved the transition to autotrophic growth, through induction of the Calvin–Benson–Bassham pathway for carbon fixation (McKinlay and Harwood, 2010), and therefore sequentially preceded autotrophic growth. The production levels paralleled growth over time (Supplementary

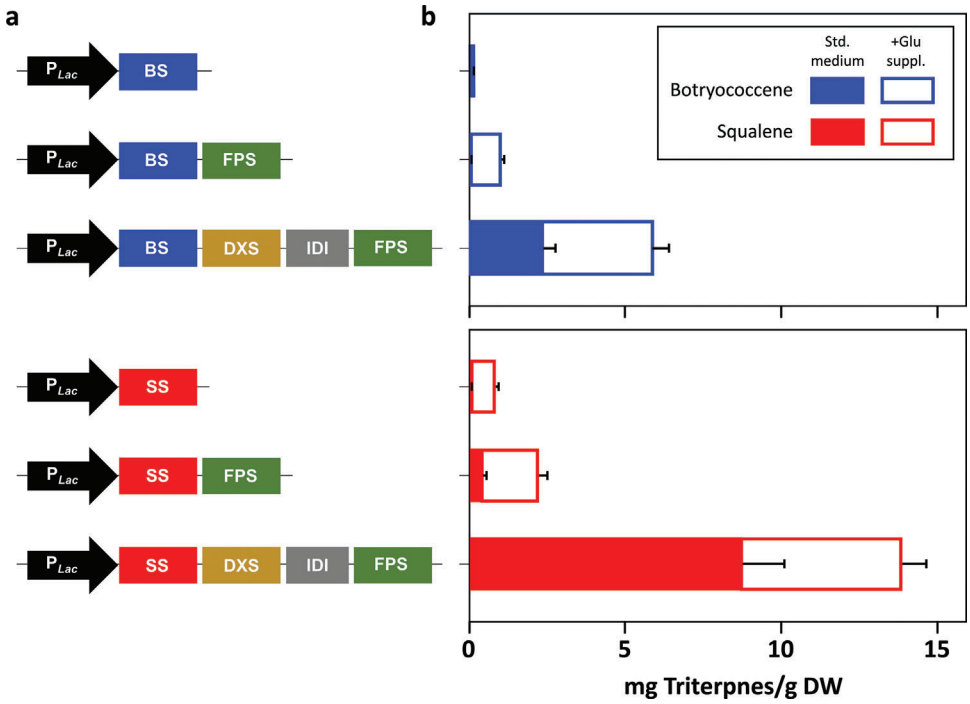

Figure 2. *Rhodobacter capsulatus* triterpene metabolic engineering. (**a**) Constructs containing botryococcene synthase (BS, upper panel) or squalene synthase (SS, lower panel) with increasing enhancements in metabolic flux by including the avian farnesyl pyrophospate synthase (*fps*), and putative rate-limiting enzymes in the MEP pathway. (**b**) Accumulation of triterpenes in *R. capsulatus* grown in standard growth medium (Std. medium) and that supplemented with an additional carbohydrate source, 80 mM glucose (+Glu suppl.) for the adjacent constructs: botryococcene for the upper panel, and squalene for the lower panel. The level of enhancement beyond standard growth medium alone is indicated by the extended bars (open bars). Experimental values were determined from five replicate cultures; error bars depict standard error of the mean.

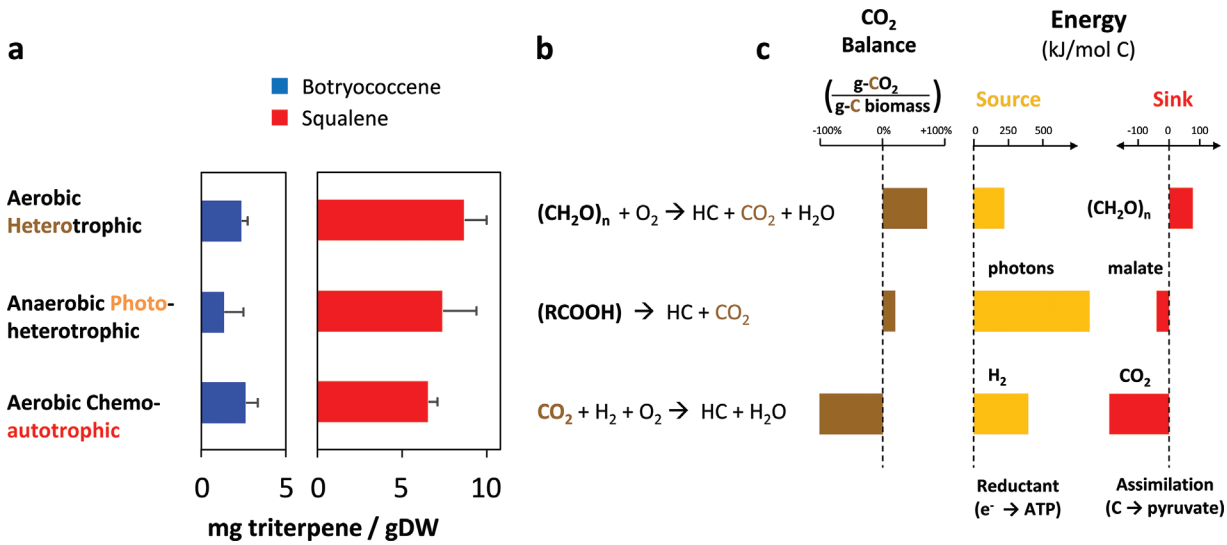

Figure 3. Exploring alternative trophisms for hydrocarbon production in *Rhodobacter*. (**a**) Triterpene specific productivity of *R. capsulatus* with pBBR:P_{lac}:BS-*dxs-idi-fps* (blue-left panel), and pBBR:P_{lac}:SS-*dxs-idi-fps* (red-right panel). (**b**) Reaction for hydrocarbon (HC) production for given tropism. (**c**) Trophims are presented quantitatively in terms of thermodynamic energy required to assimilate a mole of carbon into pyruvate as well as the energy required to produce an ATP normalized to a molar carbon basis. The carbon balance is shown to illustrate the relative magnitude of carbon produced by aerobic and photo-heterotrophic growth as compared to autotrophic CO_2 assimilation.

Figure 4) and were found to be quite similar for all three trophic growth modes for either triterpene product, with squalene levels being twofold higher than the botryococcene levels. Squalene productivity was greater than botryococcene probably because of the enzymatic efficiencies of the enzymes. Conversion of FPP to squalene is catalyzed by a single active site in the enzyme, where the conversion of FPP to pre-squalene diphosphate (PSPP) to squalene occurs without the substrate leaving the active site. In contrast, BS chimeric enzyme requires two catalytic sites, one converting FPP to PSPP, the second, PSPP to botryococcene, which would entail the release of PSPP from the active site of one enzyme and its rebinding at the second active site. These mechanisms provide an explanation for the different rates observed at similar substrate levels. Since there is a corresponding reduced accumulation of botryococcene, a degree of feedback regulation known to occur for the endogenous MEP pathway (Banerjee and Sharkey, 2014) appears to be functional in conjunction with the heterologous pathway enhancements. Although, we cannot rule out the possibility that botryococcene synthase and squalene synthase enzyme levels may also limit the overall flux. Independent of the precise rate-limiting mechanisms, obtaining similar productivities in the different trophic modes was unexpected, because the three trophic conditions represent very different physiological conditions, each having different energetic requirements. The differences for typical growth conditions in these diverse trophic modes had less impact than simple glucose supplementation. This result contrasts with the dramatically different metabolic modes (Fig. 3b) that have been quantified in the "trophism snapshots" compiled in Figure 3c. The trophisms were quantified in terms of their carbon balance, with net release of about 50% of the carbon to CO_2 in aerobic heterotrophic mode, and net capture of 100% of the CO_2 in the autotrophic mode. By comparison, about 80% of the carbon from malate ends up in the biomass for photoheterotrophic metabolism, since the ATP generation is facilitated largely by light and not from malate catabolism. The contrasting energetic features of these trophic modes are depicted in the energy "source" and "sink" values. "Source" was calculated as the efficiency with which input energy is captured as ATP. These inputs were sugar, light, and hydrogen for heterotrophic, anaerobic photoheterotrophic, and aerobic autotrophic modes of growth respectively. To place these numbers on a common carbon basis with "sink" energy requirements, a conversion factor of 2.28 mol-ATP/mol-biomass-carbon was used (Tuerk, 2011). The basis of these calculations is presented in (Supplemental Note 1). The most important features of these calculations is that the sugar, malate, and H_2 are all products of photonic energy produced externally to the production host for those alternative trophic production modes (Fig. 1). The comparable results for these dramatically different metabolisms and their associated fluxes of carbon and reducing power suggest a strong homeostatic regulation of the precursor pools of the central metabolism that is largely independent of the trophic growth mode.

Productivity Enhancement Through Bioreactor Operational Strategies

To determine if the growth-associated specific productivity could be maintained while increasing culture density through fed-batch addition of carbon and nitrogen, a typical feeding strategy of concentrated glucose feed (540 g/L) based on dissolved oxygen (DO) feedback control was implemented (Gleiser and Bauer, 1981). NH_4OH (8 N) feed was also provided for pH control while providing nitrogen (Fig. 4). The heterotrophic bioreactor culture reached an OD_{660} of 12.7 and accumulated a total of about 40 mg/L botryococcene with an average specific titer (over the entire run) of 11.7 ± 3.0 mg/gDW. This represents a twofold improvement over small scale YCC cultures with glucose supplementation, which indicates controlled pH and higher aeration significantly improved the substrate utilization of the cells to generate a greater relative flux in the MEP pathway. To provide some insight into the extent to which plasmid loss might be contributing to our observed triterpene titers despite selective pressure, we plated *R. capsulatus* pBBR:P_{lac}-*BS-dxs-idi-fps* heterotrophically grown in the bioreactor. This gave indications that as much as half of the cells might be devoid of plasmid after 70 h of growth, but acknowledge that a more in-depth study of plasmid stability is a future area of importance that goes beyond the scope of the presented work.

We expected to reach a much higher density in the heterotrophic bioreactor, but repeatedly encountered abrupt growth cessation at relatively low culture densities of less than 5 gDW/L, which are over an order-of-magnitude lower than *E. coli* cultures that routinely reach densities upwards of 100 gDW/L (Lee, 1996). We suspect that this may be a result of some form of metabolic inhibition or a quorum sensing behavior that *Rhodobacter* is known to display (Curtis, 2011; Schaefer et al., 2002). To test further, aliquots of

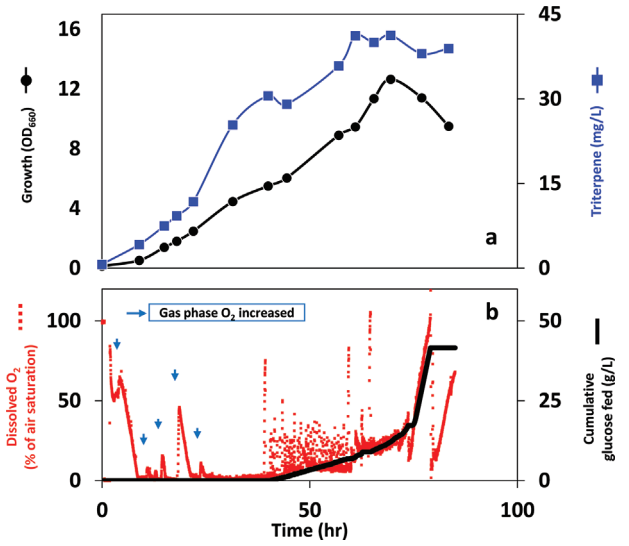

Figure 4. Heterotrophic bioreactor growth of *R. capsulatus* pBBR:P_{lac}:BS-*dxs-idi-fps*. *R. capsulatus* genetically engineered with the above expression vector was grown in a 5 L BioFlo with glucose provided as the sole carbon and energy source, followed by fed-batch supplementation based on feedback control of dissolved oxygen (DO). Ammonia was also added in a fed-batch manner for pH control. (**a**) Growth monitored as OD_{660} (black circles) and botryococcene accumulation (blue squares) respectively. (**b**) The DO (red squares) and cumulative glucose supplementation (black line), where glucose fed batch was initiated at ~40 h, and the approximate times for incremental increases in O_2 supplementation (light blue arrows) are noted. Cultures stopped growing and accumulating hydrocarbon at about 70 h; respiration slowed considerably in stationary phase as indicated by the sharp rise in DO which could not be recovered with additional glucse feed.

media from the reactor stationary phase were tested for continued growth in subsequent batch flask culture (Supplementary Figure 5). Cultures inoculated into fresh media grew robustly, whereas cultures provided with concentrated nutrients from the stationary phase bioreactor supernatant displayed minimal growth. More work would be required to determine if this is typical homoserine lactone quorum sensing behavior or a different metabolic inhibition.

Sustainable biofuel production is dependent on CO_2 fixation and we were interested in evaluating *Rhodobacter's* capacity to produce triterpene under chemoautotrophic growth. To sufficiently characterize the metabolic capacity of the *R. capsulatus* platform for triterpene production, we scaled up to a 1 L autotrophic bioreactor. *R. capsulatus* pBBR:P_{lac}::*BS-dxs-idi-fps* was grown in batch and continuous flow operation with gas phase H_2, O_2, CO_2 feeding, and NH_4OH based pH control (Fig. 5). It was found to be much more robust in terms of growth and triterpene accumulation in the scaled-up autotrophic reactor compared to heterotrophic. The inlet gas composition was manually adjusted via precise mass flow controllers to promote the high gas transport rate into the liquid (Fig. 5a). The culture reached an OD_{660} of about 17 (7 gDW/L), comparable to that attained for heterotrophic growth, yet accumulated a total of about 110 mg/L botryococcene (Fig. 5b), more than double that observed with heterotrophic reactor runs. Interestingly, in contrast to the heterotrophic bioreactor, there was a steady increase in specific triterpene level during the course of batch growth up to about 16.7 mg/gDW (Fig. 5c). The specific

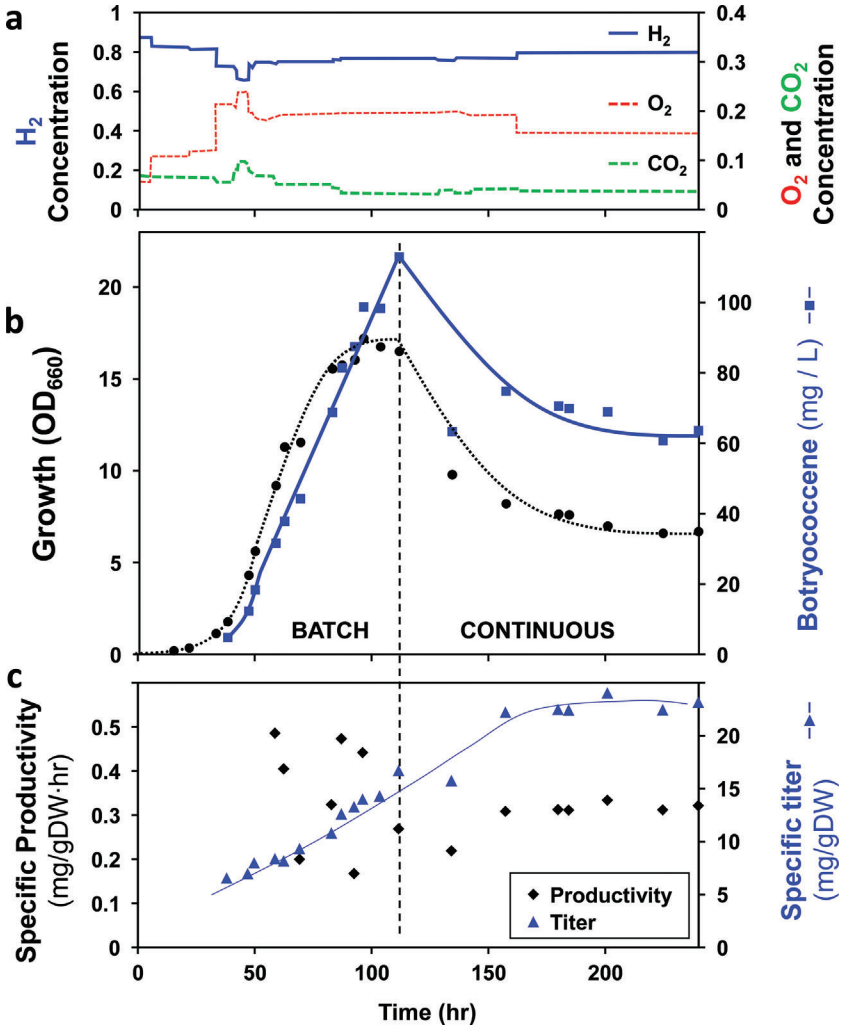

Figure 5. Performance of *R. capsulatus* pBBR:P_{lac}:BS-*dxs-idi-fps* in an autotrophic bioreactor. *R. capsulatus* expressing this plasmid was grown with gas phase feeding of H_2, O_2, and CO_2 (for growth) and liquid phase feeding of ammonia (for pH control) in batch operation for the first 110 h and under continuous operation after that. Continuous flow was established with 12.5 g/L flow of the CA medium, which corresponds to 10% of μ_{max} of *R. capsulatus*. (**a**) The inlet gas composition profile. During the batch growth mode, the compositions were varied to accommodate the growth demand, based on outlet gas composition measurement. Gas consumption did not vary greatly during continuous flow and the inlet composition was kept constant. (**b**) The OD_{660} and botryococcene profile during batch and continuous operation. Cells grew exponentially to OD 5 and linearly after that reaching a maximum of 17. Botryococcene accumulation increased proportionally as the cells and achieved a maximum volumetric accumulation of 110 mg L^{-1} botryococcene at the end of batch growth. Under continuous operation, the cells reached a steady-state within about 130 h of starting flow, reaching an OD of ~7 and maintaining a relatively constant level 60 mg L^{-1} botryococcene. (**c**) The specific botryococcene productivity profiles. The specific botryococcene levels increased steadily during batch growth to about 17 mg/gDW. Batch specific productivities were around 0.5 mg/gDWh. Specific botryococcene continued to increase during the continuous flow and reached 23 mg/gDW. However, specific productivity decreased somewhat and reached a steady level of about 0.3 mg/gDWh.

productivity of botryococcene calculated during batch growth ranged between 0.17 and 0.5 mg/gDW•h. Because steady state operation unambiguously quantifies the specific productivity, we switched the reactor to continuous operation by flowing 12.5 g/h CA medium (inorganic salts and vitamins) into the reactor and removing culture at the same rate. This corresponded to a dilution rate of $9.62 \times 10^{-3}\,h^{-1}$, roughly 10% of the maximum growth rate of *R. capsulatus* ($\mu_{max} = 0.112\,h^{-1}$). The culture density came to steady-state around 2.75 gDW/L and the specific triterpene level was found to increase further and became relatively constant at about 23 mg/gDW. The inlet gas composition was kept constant during continuous operation (Fig. 5a) to allow the culture to reach steady state. Constant outlet gas composition was obtained when the culture reached a steady state (data not shown). The steady-state triterpene specific productivity was found to be 0.32 mg/gDW•h, thereby achieving significant improvements based on all productivity measures as compared to heterotrophic small scale and reactor cultures.

Discussion

Although biofuels like ethanol and other small chain alcohols are readily obtained from genetically modified microbial hosts supplied with photosynthetic derived sugars and cellulosic feedstocks, questions remain about the sustainability and efficiency of such processes, including carbon balance and net energy generated. These observations have led to efforts aimed at coupling the production of higher energy fuel molecules to a variety of solar and geochemical energy sources. Utilizing the considerable knowledge that has become available about the bacterial MEP pathway and the biosynthesis of high-energy triterpenes, hydrocarbon biosynthetic pathways were introduced into *R. capsulatus* such that alterations in substrate availability within central metabolism through glucose feeding were reflected in enhanced triterpene accumulation.

In choosing *R. capsulatus* there was a hope that the large differences in carotenoid metabolism in these different growth modes—particularly photoheterotrophic—might provide a more favorable trophism for terpenoid flux. Carotenoids are derived from the same isoprenoid pathway intermediates as our engineered triterpenes, where levels of carotenoid estimated from literature reports are comparable (6-18 mg/gDW) (Arnheim and Oelze, 1983; Chi et al., 2014; Siefert and Pfennig, 1979) and vary with light and oxygen tension (Arnheim and Oelze, 1983). However, the observation that the levels of triterpene production were similar for fundamentally different modes of growth suggested a persistent degree of "homeostasis" existed where the pools for metabolites of central metabolism were comparable between the different trophic modes of growth and no one mode was more advantageous relative to another for hydrocarbon production. The interplay between environmental queues and the competition of endogenous and engineered pathways suggests that the inherent potential of the alternative trophisms may be obscured by endogenous regulation of the MEP pathway. Low O_2 is of particular note in the current work. The autotrophic bioreactor was maintained oxygen-limited at essentially zero dissolved oxygen and the triterpene content increased from ~5 to 23 mg/gDW at steady-state, while becoming intensely pigmented red. These observations suggest that a combination of carotenoid knockout and low oxygen tension operating conditions would be an ideal choice for follow-up research to increase productivity. In addition, follow-up work is planned to test a heterologous mevalonate (MVA) pathway that should avoid such native regulation. This MVA engineering strategy has been successful for the production of various isoprenoids in *E. coil* (Tsuruta et al., 2009).

Productivity can be enhanced considerably through bioreactor operational strategies which increase cell density while maintaining a relatively fixed triterpene content. However, this is largely limited to an order of magnitude enhancement and compliments improvements in metabolic engineering strategies.

Table I. Terpenoid productivities calculated from data reported in the literature for various systems.

Molecule	Max mg/L	Max mg/gDW	Max mg/gDW•h	Organism	Substrate/ Operation	Reference
Botryococcene (C_{30})	110	30	0.50	*R. capsulatus* (purple non-sulfur)	H_2, CO_2/Continuous (bioreactor)	This work
Botryococcene (C_{30})	4500	225	4.0	*B. braunii* Race B (algae)	Light, CO_2/Continuous (bioreactor)	Khatri et al. (2014)
Isoprene (C_5)	6300	350	9.0	*E. coli*	Complex+Glucose/ Batch (Bioreactor)	Yang et al. (2012)
β-carotene (C_{40})	390	31.7	2.63	*E. coli*	Complex/Batch (bioreactor)	Kim et al. (2006)
Lycopene (C_{40})	404	32.6	0.41	*E. coli*	Complex/Batch (shake flask)	Yoon et al. (2007)
Lycopene (C_{40})	n/a	20.8	3.13	*E. coli*	Complex/Batch (shake flask)	Farmer and Liao (2001)
Lycopene (C_{40})	n/a	18	0.72 0.38	*E. coli*	Complex/Batch (shake flask) Complex/Batch (bioreactor)	Alper et al. (2005)
Amorphadiene (C_{15})	7.78	13.0	1.84	*E. coli*	Complex/Batch (shake flask)	Martin et al. (2003)
Amorphadiene (C_{15})	27400	304	12.7	*E. coli*	Glucose/Batch (bioreactor)	Tsuruta et al. (2009)
Amorphadiene (C_{15})	40000	500	7.14	*S. cerevisiae*	Glucose/Batch (bioreactor)	Westfall (2012)
Astaxanthin (C_{40})	8.9	1.1	0.052	*Methylomonas sp. 16a* (methanotroph)	Methane/Batch (shake flask)	Ye et al. (2007)
Astaxanthin (C_{40})	n/a	11.6	0.365	*Haematococcus pluvialis* (marine algae)	Light, acetate/Batch (shake flask)	Steinbrenner and Sandmann (2006)

A comparison of this work to other efforts at terpene hydrocarbon metabolic engineering is very informative as compiled in Table I, most of which are based on complex carbon source or sugars. The maximum specific productivity in this work of 0.5 mg/gDW•h is on par with several lycopene (C_{40}) tetraterpene efforts, however, the distinct advantage of high-throughput screening for colored compounds has allowed for selecting production levels of both lycopene and carotene to about 3 mg/gDW•h. By comparison, the production rates of ethanol are on the order of 500 mg/gDW•h (estimated from (Ohta et al., 1991), which illustrates the challenge of competing with a pathway that is a natural obligatory final electron acceptor. What is most surprising, is a comparison to the native *Botryococcus braunii* algae, where recent continuous culture work has provided very accurate specific productivity levels at 4 mg/gDW•h (Khatri et al., 2014) which represents photosynthetic conditions from an organism that is notoriously slow growing (doubling times of 4 + days). This terpenoid flux has only been exceeded by the recent work using a modified MVA pathway to produce amorphadiene (C_{15}) at ~13 mg/gDW•h in *E. coli* fed with glucose (Tsuruta et al., 2009). Combined with the comparative achievements of modest production levels, suggests that there are critical aspects of metabolic engineering of hydrocarbons that remain to be discovered. It is also interesting that the native algae biochemistry produces nearly exclusively tetra-methyl-botryococcene. This suggests that there is sub-cellular management of carbon flux that will likely require intricate recapitulation in heterologous hosts to achieve high stable hydrocarbon production. Although organisms with alternative trophic modalities are more difficult to work with experimentally, the results presented here demonstrate a comparable potential for biochemicals production that do not rely on sugar as a carbon source.

We thank Dr. Joseph Perez for upgrade support of GC analysis capability. Assistance with culturing and molecular biology was provided by Alex S. Rajangam, Mustafa Erbakan, Justin Yoo, William Muzika, Ben Woolston, Brandon S. Curtis, and Stephanie Tran. Ryan Johnson provided assistance with analytics development as well as bioreactor instrumentation. We thank Jennifer Curtis for generating drawings for Figure 1. This work was funded by an ARPA-e grant from the U.S. Department of Energy (ARPA-e Electrofuels, #DE-AR0000092) to W.R.C. and J.C. The multi-trophic concept was developed by W.R.C. in discussions with Brandon Curtis. J.C. developed the molecular biology strategy; S.E.N. fabricated the constructs. N.K. performed bioreactor runs and energetics calculations with W.R.C. License agreements are being developed between UK and TerGen Biotechnology, Inc., and J.C. has an equity stake in TerGen. W.R.C. is the sole proprietor of CALYX Bioprocessing, LLC, which was established to help support bioprocessing commercialization and consulting efforts.

References

Alper H, Miyaoku K, Stephanopoulos G. 2005. Construction of lycopene-overproducing *E. coli* strains by combining systematic and combinatorial gene knockout targets. Nat Biotechnol 23:612–616. http://www.ncbi.nlm.nih.gov/pubmed/15821729

Arnheim K, Oelze J. 1983. Differences in the control of bacteriochlorophyll formation by light and oxygen. Arch Microbiol 135(4):299–304. Available at: http://link.springer.com/10.1007/BF00413485 [Accessed January 13, 2015]

Banerjee A, Sharkey TD. 2014. Methylerythritol 4-phosphate (MEP) pathway metabolic regulation. Nat Prod Rep 31:1043–1055. http://www.ncbi.nlm.nih.gov/pubmed/24921065

Bongers L. 1970. Energy generation and utilization in hydrogen bacteria. J Bacteriol 104:145–151. http://www.pubmedcentral.nih.gov/articlerender.fcgi?artid=248194&tool=pmcentrez&rendertype=abstract

Chi SC, Mothersole DJ, Dilbeck P, Niedzwiedzki DM, Zhang H, Qian P, Vasilev C, Grayson KJ, Jackson PJ, Martin EC, Li Y, Holten D, Neil Hunter C. 2014. Assembly of functional photosystem complexes in *Rhodobacter sphaeroides* incorporating carotenoids from the spirilloxanthin pathway. Biochim Biophys Acta 1847(2):189–201. Available at: http://www.ncbi.nlm.nih.gov/pubmed/25449968 [Accessed January 7, 2015]

Curtis B. 2011. (Thesis) Development of *Rhodobacter* for the production of functional membrane proteins. The Pennsylvania State University. https://honors.libraries.psu.edu/paper/1965/

Derenne S, Largeau C, Hetényi M, Brukner-Wein A, Connan J, Lugardon B. 1997. Chemical structure of the organic matter in a Pliocene maar-type shale: Implicated Botryococcus race strains and formation pathways. Geochim Cosmochim Acta 61:1879–1889. http://www.sciencedirect.com/science/article/pii/ S0016703797000422

Farmer WR, Liao JC. 2001. Precursor balancing for metabolic engineering of lycopene production in *Escherichia coli*. Biotechnol Prog 17:57–61. http://www.ncbi.nlm.nih.gov/pubmed/11170480

Gleiser I, Bauer S. 1981. Growth of *E. coli* W to high cell concentration by oxygen level linked control of carbon source concentration. Biotechnol Bioeng XXIII:1015–1021. http://onlinelibrary.wiley.com/doi/10.1002/bit.260230509/abstract

Glikson M, Lindsay K, Saxby J. 1989. *Botryococcus*—A planktonic green alga, the source of petroleum through the ages: Transmission electron microscopical studies of oil shales and petroleum source rocks. Org Geochem 14:595–608. http://www.sciencedirect.com/science/article/pii/0146638089900399

Hillen LW, Pollard G, Wake LV, White N. 1982. Hydrocracking of the oils of *Botryococcus braunii* to transport fuels. Biotechnol Bioeng 24:193–205. http://www.ncbi.nlm.nih.gov/pubmed/18546110

Imam S, Noguera DR, Donohue TJ. 2013. Global insights into energetic and metabolic networks in *Rhodobacter sphaeroides*. BMC Syst. Biol 7:89. http://www.pubmedcentral.nih.gov/articlerender.fcgi?artid=3849096&tool=pmcentrez&rendertype=abstract

Khatri W, Hendrix R, Niehaus T, Chappell J, Curtis WR. 2014. Hydrocarbon production in high density *Botryococcus braunii* race B continuous culture. Biotechnol Bioeng 111:493–503. http://www.ncbi.nlm.nih.gov/pubmed/24122424

Kim S-W, Kim J-B, Jung W-H, Kim J-H, Jung J-K. 2006. Over-production of beta-carotene from metabolically engineered *Escherichia coli*. Biotechnol Lett 28:897–904. http://www.ncbi.nlm.nih.gov/pubmed/16786275

Lee SY. 1996. High cell-density culture of *Escherichia coli*. Trends Biotechnol 14:98–105. http://www.ncbi.nlm.nih.gov/pubmed/8867291

Madigan M, Gest H. 1979. Growth of the photosynthetic bacterium *Rhodopseudomonas capsulata* chemoautotrophically in darkness with H2 as the energy source. J Bacteriol 137:524–530. http://jb.asm.org/content/137/1/524.short

Martin VJJ, Pitera DJ, Withers ST, Newman JD, Keasling JD. 2003. Engineering a mevalonate pathway in *Escherichia coli* for production of terpenoids. Nat Biotechnol 21:796–802. http://www.ncbi.nlm.nih.gov/pubmed/12778056

McKinlay JB, Harwood CS. 2010. Carbon dioxide fixation as a central redox cofactor recycling mechanism in bacteria. Proc Natl Acad Sci USA 107:11669–11675.

Metzger P, Largeau C. 2005. *Botryococcus braunii*: a rich source for hydrocarbons and related ether lipids. Appl Microbiol Biotechnol 66:486–496. http://www.ncbi.nlm.nih.gov/pubmed/15630516

Miller B, Heuser T, Zimmer W. 2000. Functional involvement of a deoxy-D-xylulose 5-phosphate reductoisomerase gene harboring locus of *Synechococcus leopoliensis* in isoprenoid biosynthesis. FEBS Lett 481:221–226. http://www.ncbi.nlm.nih.gov/pubmed/11007968

Niehaus TD, Okada S, Devarenne TP, Watt DS, Sviripa V, Chappell J. 2011. Identification of unique mechanisms for triterpene biosynthesis in *Botryococcus braunii*. Proc Natl Acad Sci USA 108:12260–12265. http://www.pubmedcentral.nih.gov/articlerender.fcgi?artid=3145686&tool=pmcentrez&rendertype=abstract

Ohta K, Beall D, Mejia J, Shanmugam K, Ingram L. Genetic improvement of *Escherichia coli* for ethanol production: chromosomal integration of *Zymomonas mobilis* genes encoding pyruvate decarboxylase and alcohol.

Appl Environ Microbiol 57:893–900. http://aem.asm.org/content/57/4/893.short

Schaefer AL, Taylor TA, Beatty JT, Greenberg EP. 2002. Long-chain acyl-homoserine lactone quorum-sensing regulation of *Rhodobacter capsulatus* gene transfer agent production. J Bacteriol 184:6515–6521. http://jb.asm.org/content/184/23/6515.shorts

Schmidt CO, Bouwmeester HJ, Bülow N, König WA. 1999. Isolation, characterization, and mechanistic studies of (−)-alpha-gurjunene synthase from *Solidago canadensis*. Arch Biochem Biophys 364:167–177. http://www.ncbi.nlm.nih.gov/pubmed/10190971

Siefert E, Pfennig N. 1979. Chemoautotrophic growth of *Rhodopseudomonas* species with hydrogen and chemotrophic utilization of methanol and formate. Arch Microbiol 122(2):177–182. Available at: http://www.springerlink.com/index/V323851512727030.pdf [Accessed June 3, 2011]

Simon R, Priefer U, Pühler A. 1983. A broad host range mobilization system for in vivo genetic engineering: transposon mutagenesis in gram negative bacteria. Nat Biotechnol 1:784–791. http://www.nature.com/nbt/journal/v1/n9/abs/n1183–784.html

Sistrom WR. 1977. Transfer of chromosomal genes mediated by plasmid r68. 45 in *Rhodopseudomonas sphaeroides* J Bacteriol 131(2):526–532

Steinbrenner J, Sandmann G. 2006. Transformation of the green alga *Haematococcus pluvialis* with a phytoene desaturase for accelerated astaxanthin biosynthesis. Appl Environ Microbiol 72:7477–7484. http://www.pubmedcentral.nih.gov/articlerender.fcgi?artid=1694260&tool=pmcentrez&rendertype=abstract

Tsuruta H, Paddon CJ, Eng D, Lenihan JR, Horning T, Anthony LC, Regentin R, Keasling JD, Renninger NS, Newman JD. 2009. High-level production of amorpha-4, 11-diene, a precursor of the antimalarial agent artemisinin, in *Escherichia coli*. PLoS ONE 4:e4489.

Tuerk A. (Thesis) 2011. An assessment of photosynthetic biofuels and electrofuels technologies under rate-limited conditions. The Pennsylvania State University. https://etda.libraries.psu.edu/paper/12318/

Westfall PJ. 2012. Production of amorphadiene in yeast, and its conversion to dihydroartemisinic acid, precursor to the antimalarial agent artemisinin. Proc Natl Acad Sci USA 109:E111–E118.

Wu S, Jiang Z, Kempinski C, Eric Nybo S, Husodo S, Williams R, Chappell J. 2012. Engineering triterpene metabolism in tobacco. Planta 236:867–877. http://www.pubmedcentral.nih.gov/articlerender.fcgi?artid=3810399&tool=pmcentrez&rendertype=abstract

Wu S, Schalk M, Clark A, Miles RB, Coates R, Chappell J. 2006. Redirection of cytosolic or plastidic isoprenoid precursors elevates terpene production in plants. Nat Biotechnol 24:1441–1447. http://dx.doi.org/10.1038/nbt1251

Yang J, Xian M, Su S, Zhao G, Nie Q, Jiang X, Zheng Y, Liu W. 2012. Enhancing production of bio-isoprene using hybrid MVA pathway and isoprene synthase in *E. coli*. PLoS ONE 7:e33509. http://www.pubmedcentral.nih.gov/articlerender.fcgi?artid=3338741&tool=pmcentrez&rendertype=abstract

Ye RW, Yao H, Stead K, Wang T, Tao L, Cheng Q, Sharpe PL, Suh W, Nagel E, Arcilla D, Dragotta D, Miller ES. 2007. Construction of the astaxanthin biosynthetic pathway in a methanotrophic bacterium *Methylomonas* sp. strain 16a. J Ind Microbiol Biotechnol 34:289–299. http://www.ncbi.nlm.nih.gov/pubmed/17205350

Yoon S-H, Kim J-E, Lee S-H, Park H-M, Choi M-S, Kim J-Y, Lee S-H, Shin Y-C, Keasling JD, Kim S-W. 2007. Engineering the lycopene synthetic pathway in *E. coli* by comparison of the carotenoid genes of *Pantoea agglomerans* and *Pantoea ananatis*. Appl Microbiol Biotechnol 74:131–139. http://www.ncbi.nlm.nih.gov/pubmed/17115209

Supporting Information

Additional supporting information may be found in the online version of this article at the publisher's web-site.